Absorption and emission spectroscopy of Eu^{3+} in metaphosphate glasses

J. A. Capobianco and P. P. Proulx
Department of Chemistry and Biochemistry, Concordia University, 1455 de Maisonneuve Blvd. West, Montréal, Québec, Canada H3G 1M8

M. Bettinelli and F. Negrisolo
Dipartimento di Chimica Inorganica, Metallorganica ed Analitica, Universitá di Padova, Via Loredan 4, 35131, Padua, Italy

(Received 20 April 1990; revised manuscript received 11 June 1990)

Optical absorption and emission spectra of Eu^{3+} in $Ba(PO_3)_2$, $Zn(PO_3)_2$, and $Pb(PO_3)_2$ glasses are reported. Judd-Ofelt intensity parameters for f-f transitions were derived from the integrated absorption spectra and used to calculate the spontaneous emission probabilities from the $^5D_0$ state. Fluorescence-line-narrowed emission excited by the $^5D_0 \leftarrow {}^7F_0$ transition was used to study local structure around the Eu^{3+} ion. A phenomenological crystal-field analysis was conducted using C_{2v} symmetry, and it was found that the sites occupied by Eu^{3+} in the glasses are adequately described by Brecher and Riseberg's model. The influence of the network modifier ions (Ba, Zn, and Pb) on the major crystal-field parameter ratio (B_{22}/B_{20} and B_{44}/B_{40}) is discussed. Furthermore, it was shown that the network modifier ions affect the properties of the Eu—O bond, and, consequently, the crystal-field strength.

I. INTRODUCTION

Extensive investigations of the luminescent properties of the Eu^{3+} ion in oxide glasses[1–6] have shown that the Eu^{3+} emission spectrum can be affected by varying the glass composition. For example, the $^5D_0 \rightarrow {}^7F_2$ transition probability has been shown to be very sensitive to relatively small changes in the chemical surrounding of the Eu^{3+} ion.[7–9] A large transition probability of the aforementioned transition has been postulated to be due to an increase in covalency[10–12] (decreasing electronegativity of glass), which is mainly determined by the network forming ions. On the other hand, network modifiers cause slight deviation of the local environment around the fluorescent ion (usually low concentration of a rare-earth ion that has been included in the glass). In either case, knowledge of the symmetry and bonding of the probe ion (Eu^{3+}) and how they vary with chemical composition of the glass and from site to site throughout the glass are essential to understanding the atomic scale structure of glass.[13] Optical spectroscopy (absorption, emission, fluorescence line narrowing) and crystal-field analysis are particularly useful in this aspect. Eu^{3+} has been the favorite probe ion to study because of the relative simplicity of its energy-level structure and the fact that it possesses nondegenerate ground ($^7F_0$) and emitting states ($^5D_0$).

The aim of this research is a detailed study of the optical properties exhibited by trivalent europium in barium, zinc, and lead metaphosphate glasses. The subject is covered in four parts. First, absorption spectra and fluorescence lifetimes of Eu^{3+} ions were measured for the following polymeric phosphate glasses: $[M(PO_3)_2]_n$, where M=Ba, Zn, Pb. Second, Judd-Ofelt parameters for the f-f transitions were derived from the integrated absorption spectra and used to calculate the spontaneous emission probabilities from the $^5D_0$ state. Third, fluorescence line narrowing (FLN) or site selective spectroscopy was used to study the local environment around the fluorescent ion (Eu^{3+}). Finally, a phenomenological crystal-field analysis of the spectral data was carried out to obtain information regarding local site symmetry and properties of the chemical bonding.

II. EXPERIMENT

Metaphosphate glasses of composition $M(PO_3)_2$ (where M= Ba, Zn, or Pb) doped with 2.5 mol % of $Eu(PO_3)_3$ were investigated. The samples were prepared by mixing appropriate quantities of PbO (Carlo Erba RPE), $(NH_4)_2HPO_4$ (Carlo Erba RPE, ZnO (Jannsen Reagent Grade), $BaCO_3$ (Merck Reagent Grade) in a ceramic crucible [for $Pb(PO_3)_2$], or in a sintered alumina crucible [for $ZnPO_3)_2$ and $Ba(PO_3)_2$]. The compositions were melted for: 2 hr. at 1250 °C [$Zn(PO_3)_2$], 900 °C [$Pb(PO_3)_2$], and 1200 °C [$Ba(PO_3)_2$]. Each melt was then cast in a stainless steel mold and annealed for 12 h at temperatures close to their softening points. Samples were cut to a 0.3–1.0 cm thickness and carefully polished for the optical measurements.

Absorption spectra of Eu^{3+} in the range 250–900 nm were recorded for all glasses at 293 K with a Perkin Elmer Lambda 15 spectrophotometer (spectral resolution, 1 nm). Low-resolution europium fluorescence spectra were recorded at 293 K in the visible region with a Perkin Elmer MPF 44 corrected fluorimeter. Fluorescence decays were measured at 293 K using a Perkin Elmer LS5 fluorimeter equipped with a broad-band radiation source. The third e-folding times of the $^5D_0$ decay were measured. In this time interval the decay curves were exactly

exponential; however, the presence of a slow decay component cannot be excluded.

A Spectra Physics 375 dye laser operating with rhodamine 6G (10^{-3} mol/dm^3 in ethylene glycol) pumped by a Coherent CR-18 argon-ion laser was used for excitation of the FLN spectra. The laser has a typical linewidth of 2 cm^{-1} full width at half maximum (FWHM) over the tuning range 575 to 581 nm used in this work. Emission spectra were excited directly with the 514.5 nm green line of the argon-ion laser. All FLN spectra were recorded with a Jarrell-Ash 1-m Czerny-Turner double monochromator using a maximum slit of 100 μm. The fluorescence signal was monitored with an RCA-C31034-02 photomultiplier operating in the photon counting mode and recorded under computer control using a Stanford SR 465 software data acquisition/analysis system. The data was acquired at liquid nitrogen temperature (77 K) using an Oxford Instruments continuous flow cryostat (CF 204).

Energy levels were determined by deconvoluting the measured spectra with a Gaussian band least-squares minimization routine[14] employing a Marquardt algorithm.[15] The crystal-field parameters, B_{nm}, were obtained using the equations for C_{2v} symmetry given by Lempicki *et al.*[16] and determined by successive approximation using the program C2V–Fit.[14] This program uses a simplex algorithm to minimize the sum of squared residuals between the observed and fitted energy levels. The program accepts as input the observed peak positions of the eight crystal-field components of the $^7F_1$ and $^7F_2$ multiplets. It assigns the symmetries to the peaks in the order A_2, B_1, B_2 for $^7F_1$ and B_1, A_1, B_2, A_2, and A_1 for $^7F_2$.

III. RESULTS

A. Absorption and fluorescence spectroscopy

Figure 1 shows the room-temperature absorption spectra of the glasses under investigation in the range 350–600 nm. They consist of several inhomogeneously broadened transitions from the $^7F_0$ ground state and the thermally populated $^7F_1$ state (whose barycenter lies at approximately 360–390 cm^{-1} above the $^7F_0$) to the excited states belonging to the $4f^6$ configuration. The transition energies are similar to those measured for Eu^{3+} in other oxide glasses.[1–5] The $f \rightarrow f$ transitions are obscured by a rapidly rising background at energies higher than 27 000 cm^{-1} for $Zn(PO_3)_2$ and 28 500 cm^{-1} for $Pb(PO_3)_2$ and $Ba(PO_3)_2$. The presence of this cutoff limits the number of absorption transitions that can be observed. Attempts to measure the $^7F_6 \leftarrow {}^7F_0$ transition in the 2.0 μm region were unsuccessful due to severe scattering. The bands in Fig. 1 correspond to transition from the $^7F_0$ ground state, and the thermally populated $^7F_1$ to the $[SL]J$ states listed in Table I.

The low-resolution room-temperature fluorescence spectra excited at 394 nm ($^5L_6 \leftarrow {}^7F_0$) showed inhomogeneously broadened $^5D_0 \rightarrow {}^7F_J (J=0-4)$ transitions. The $^7F_{5,6}$ transitions were outside our experimental range and could not be measured. Evidence of a weak and broad

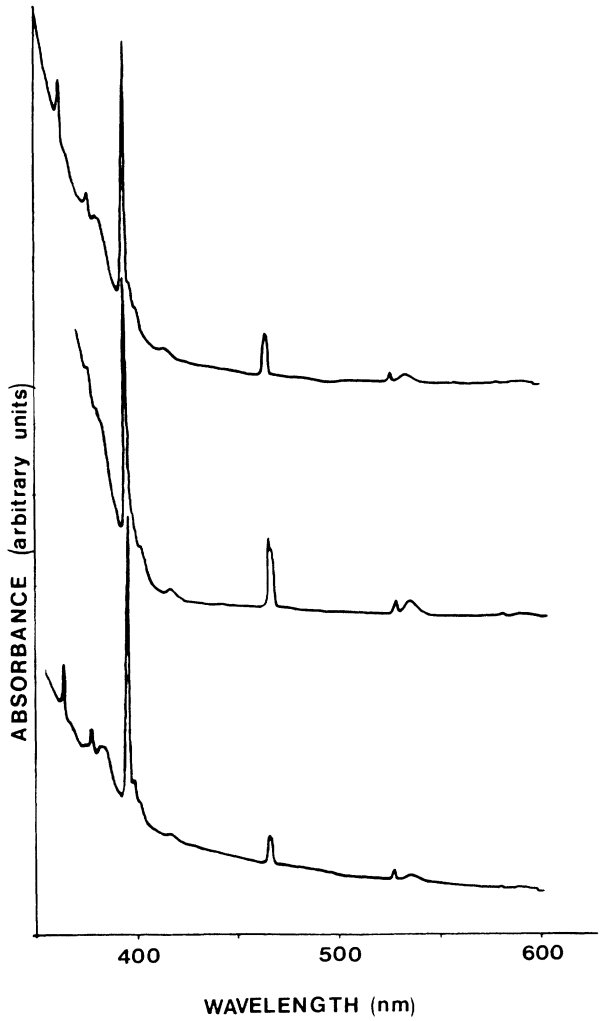

FIG. 1. Absorption spectra at 293 K of Eu^{3+} in $Ba(PO_3)_2$ (top), $Zn(PO_3)_2$ (middle) and $Pb(PO_3)_2$ (bottom) glasses.

emission around 400 nm was detected in the Eu^{3+} doped $Zn(PO_3)_2$ glasses excited at 320 nm. We assigned this emission to allowed interconfigurational transition of Eu^{2+} present in trace amounts in the glasses prepared at higher temperture (≥ 1200 °C).

B. Transition intensities

The transitions responsible for the bands in the absorption and fluorescence spectra can be accounted for by a magnetic or a forced electric dipole mechanism. The oscillator strength, P, of the forced electric dipole transition can be expressed in terms of three phenomenological parameters, Ω_t on the basis of the Judd-Ofelt theory[17,18]

$$P = \frac{8\pi mc\sigma}{3h(2J+1)} \frac{(n^2-2)^2}{9n} \sum_{t=2,4,6} \Omega_t |U^t|^2 , \quad (1)$$

where $(2J+1)$ is the multiplicities of the lower states; n is the refractive index; m is the mass of the electron and σ is the peak absorption (wave number). The Judd-Ofelt parameters Ω_2, Ω_4, and Ω_6 were calculated from the

TABLE I. Position and assignment of bands for the absorption spectra of $Zn(PO_3)_2$, $Pb(PO_3)_2$, and $Ba(PO_3)_2$ at 293 K. Oscillator strengths P_c, corrected for the thermal population for the transitions from the $^7F_0$ levels are reported. (a) indicates a barely observable value. Parentheses around an actual value indicates a shoulder.

	$Zn(PO_3)_2$		$Pb(PO_3)_2$		$Ba(PO_3)_2$	
Assignment	bary-center (cm^{-1})	$P_c(10^{-7})$	bary-center (cm^{-1})	$P_c(10^{-7})$	bary-center (cm^{-1})	$P_c(10^{-7})$
$^5D_0 \leftarrow ^7F_0$	17 316	(a)				
$^5D_1 \leftarrow ^7F_1$	18 797		18 762		18 797	
$^5D_1 \leftarrow ^7F_0$	19 011	0.18	19 011	0.21	18 975	0.22
$^5D_2 \leftarrow ^7F_0$	21 528	2.19	21 505	1.36	21 505	2.19
$^5D_3 \leftarrow ^7F_0$	24 125	0.32	(24 150)		(24 150)	
$^5L_6 \leftarrow ^7F_1$	25 031		25 062		(25 060)	
$^5L_6 \leftarrow ^7F_0$	25 413	7.90	25 413	13.30	25 413	11.10
$^5L_7 \leftarrow ^7F_1$			26 180			
$^5G_2 \leftarrow ^7F_1$	(26 390)				(26 390)	
$^5G_5 \leftarrow ^7F_1$						
$^5G_6$						
$^5G_4 \leftarrow ^7F_0$	(26 650)		26 596	0.92	(26 670)	
$^5G_5$						
$^5D_4 \leftarrow ^7F_0$			27 624	2.12	(27 620)	

emission and absorption spectra and using the matrix elements of Weber[19] and Carnall *et al.*,[20] respectively. The Judd-Ofelt parameters obtained for the samples are tabulated in Table II.

The spontaneous emission probability, A, was calculated from the Judd-Ofelt parameters using the following equation:

$$A = \frac{64\pi^2 e^2 \sigma^3}{3h(2J+1)} \frac{n(n^2+2)^2}{9} \sum_{t=2,4,6} \Omega_t |U^t|^2 , \qquad (2)$$

where $2J^1+1$ is the multiplicity of the upper state, n is the refractive index; e is the electron charge; and σ is the peak fluorescence (wave number). The spontaneous radiative transition probabilities are reported in Table III.

The fluorescence lifetimes for the $^5D_0 \rightarrow ^7F_0$ transitions measured at 293 K for $Zn(PO_3)_2$, $Pb(PO_3)_2$, and $Ba(PO_3)_2$, were found to be 2.3, 2.0, and 2.3 ms, respectively. The highest vibrational frequency in phosphate glasses is about 1200 cm^{-1} therefore it is reasonable to assume that the quantum efficiency of the emission from the $^5D_0$ is close to unity. The radiative lifetimes of the $^5D_0$ calculated from the spontaneous radiative transition probabilities are included at the bottom of Table III. They were found to be comparable to the observed fluorescence lifetimes.

C. Site selective spectroscopy

Figure 2 shows the low-temperature (77 K) $^5D_0 \rightarrow ^7F_0$, $^7F_1$, $^7F_2$ region of the Eu^{3+} emission spectra excited at 514.5 nm from the barium (top), zinc (middle), and lead (bottom) metaphosphate glasses. The broad inhomogeneous profile for the $^5D_0 \rightarrow ^7F_0$ transition in each of the metaphosphate glasses at 77 K arises from the site-to-site variations of the crystal-field strength. The full widths at half maximum for the transition $^5D_0 \rightarrow ^7F_0$, were found to be 46 cm^{-1}, 56 cm^{-1}, and 66 cm^{-1} for $Pb(PO_3)_2$, $Ba(PO_3)_2$, and $Zn(PO_3)_2$, respectively, and are much narrower in comparison to those reported for oxide glasses that are usually about 100 cm^{-1}.[1-6] Despite the general similarity of the $^5D_0 \rightarrow ^7F_0$ emission band for the three samples the line shape for the barium and zinc metaphos-

TABLE II. Judd-Ofelt parameters Ω_t, for Eu^{3+} in $Zn(PO_3)_2$, $Pb(PO_3)_2$, $Ba(PO_3)_2$ glasses.

Host	$\Omega_2(10^{-20}$ $cm^2)$	$\Omega_4(10^{-20}$ $cm^2)$	$\Omega_6(10^{-20}$ $cm^2)$
$Zn(PO_3)_2$	7.4±1.6[a]	2.3[b]	1.3[c]
$Pb(PO_3)_2$	4.3±0.5[a]	3.1±0.9[b]*	2.0[c]
$Ba(PO_3)_2$	5.9±3.2[a]	1.4[b]	1.8[c]

[a]Determined from the transitions $^5D_2 \leftarrow ^7F_0$ and $^5D_0 \rightarrow ^7F_2$.
[b]Determined from the transitions $^5D_0 \rightarrow ^7F_4$* $^5G_4 \leftarrow ^7F_0$ and $^5D_4 \leftarrow ^7F_0$.
[c]Determined from the transitions $^5L_6 \leftarrow ^7F_0$.

TABLE III. Calculated spontaneous emission probabilities, A, at 293 K for the transitions $^5D_0 \rightarrow ^7F_J$ ($J=1-4$). Calculated fluorescence lifetimes (τ) of the $^5D_0$.

Assignment	$Zn(PO_3)_2$ A (s^{-1})	$Pb(PO_3)_2$ A (s^{-1})	$Ba(PO_3)_2$ A s^{-1})
$^5D_0 \rightarrow ^7F_1$	51.3	75.2	58.4
$^5D_0 \rightarrow ^7F_2$	300.0	253.4	262.8
$^5D_0 \rightarrow ^7F_3$			5.6
$^5D_0 \rightarrow ^7F_4$	45.7	94.1	31.0
τ_{calc}(ms)	2.5	2.4	2.8

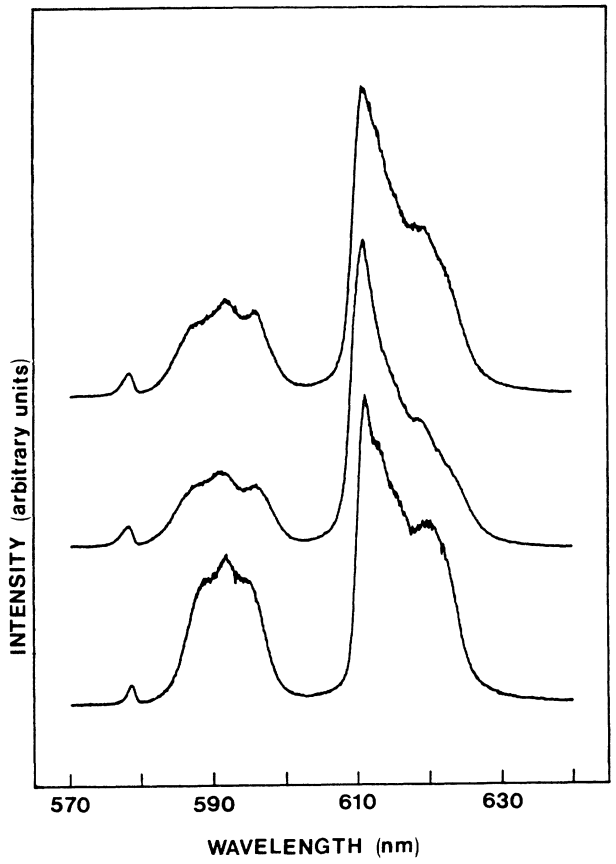

FIG. 2. Emission spectra of Eu^{3+} in $Ba(PO_3)_2$ (top), $Zn(PO_3)_2$ (middle), and $Pb(PO_3)_2$ (bottom) glasses. Excited at 514.5 nm and observed at 77 K.

phate glasses show more asymmetry (high-energy side) than the lead metaphosphate, and the peak maxima shifted to lower energy in the following order: Zn metaphosphate, (17 291 cm^{-1}) Ba metaphosphate (17 286 cm^{-1}) and Pb metaphosphate (17 276 cm^{-1}).

One immediately evident feature is the dominance (intensity) of the $^5D_0 \rightarrow {}^7F_2$ electric dipole transition for the zinc and barium metaphosphate glasses. However, this hypersensitive transition ($^5D_0 \rightarrow {}^7F_2$) is slightly suppressed for the lead metaphosphate glass. This behavior is characterized by the relatively lower Judd-Ofelt intensity parameter Ω_2 (Table II) for lead metaphosphate. For the $^5D_0 \rightarrow {}^7F_1$ transition we observe three broad overlapping lines in the regions 580.4−602.9 nm, 580.1−602.4 nm, and 580−603.4 nm for Pb, Ba, and Zn metaphosphate, respectively, corresponding to emission to the three Stark components of the $^7F_1$ state. The linewidths of each component is about 177 cm^{-1}, 184 cm^{-1}, and 153 cm^{-1} for Ba, Zn, and Pb metaphosphate, respectively. For each of the $^5D_0 \rightarrow {}^7F_2$ transitions, a broad incompletely resolved band containing the five Stark components is seen (603–638 nm). The full width is about 730 cm^{-1}, for the three glasses.

Figures 3, 4, and 5 show the line narrowed emission spectra of the barium, zinc, and lead metaphosphate

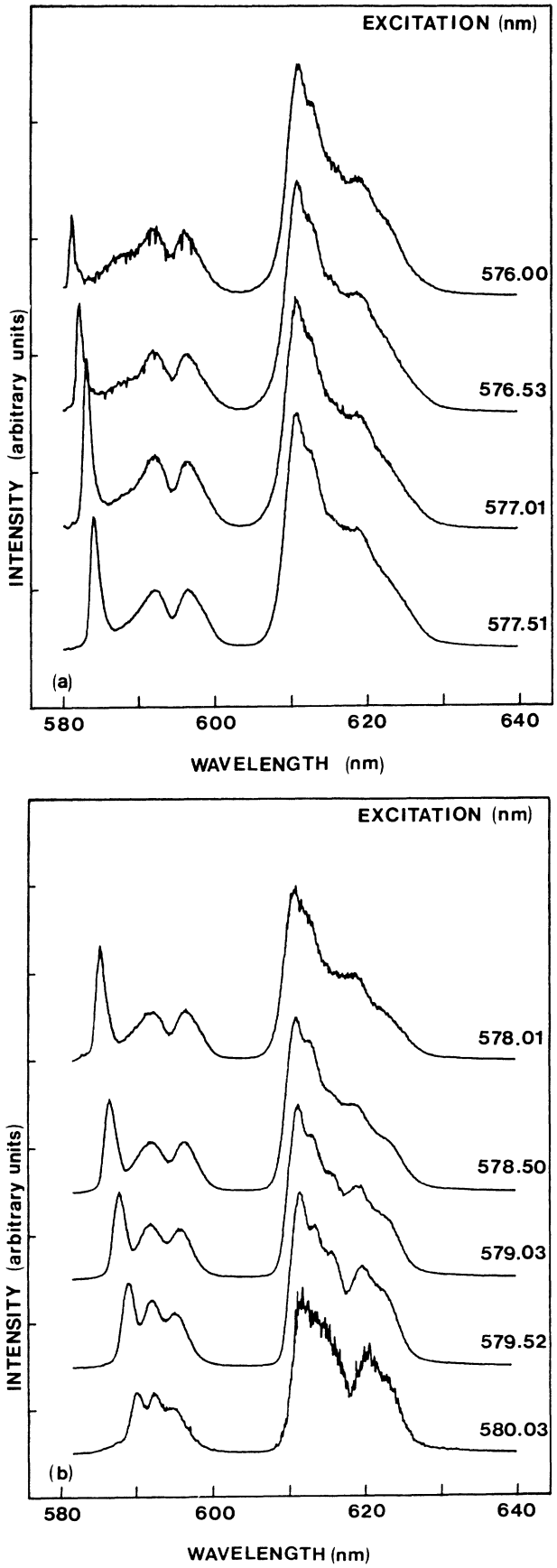

FIG. 3. Emission spectra of Eu^{3+} in $Ba(PO_3)_2$ glass at 77 K using different excitation wavelengths.

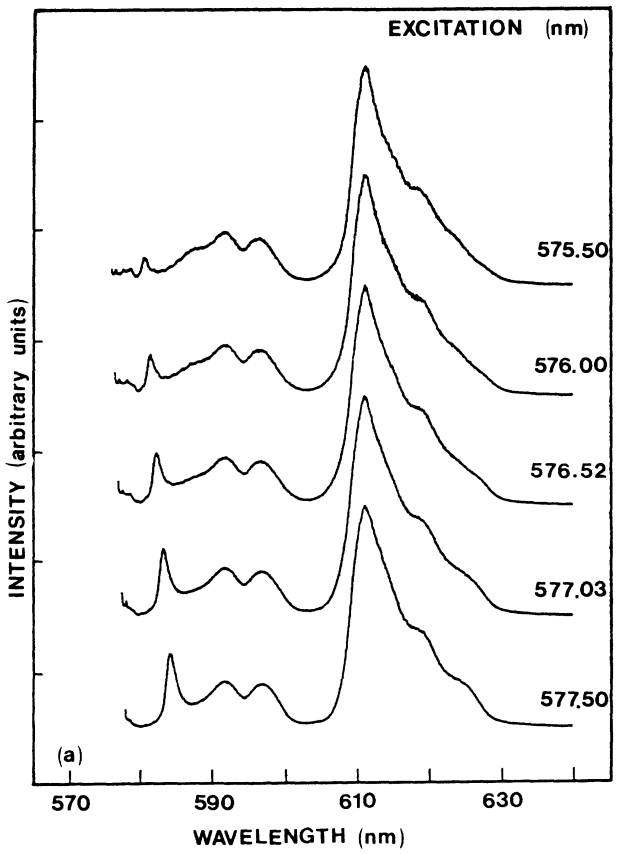

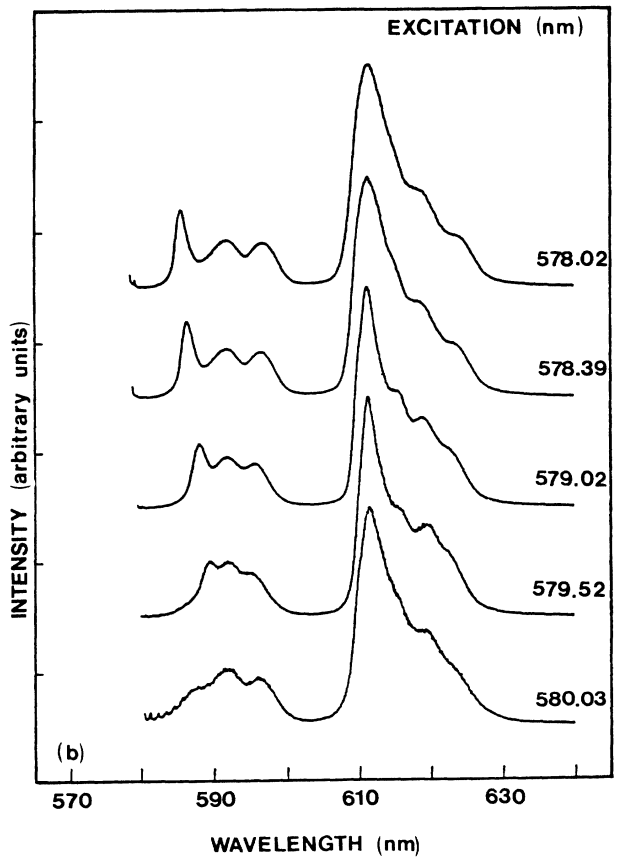

FIG. 4. Emission spectra of Eu^{3+} in $Zn(PO_3)_2$ at 77 K using different excitation wavelengths.

glasses, respectively, excited at various wavelengths within the $^5D_0 \rightarrow {}^7F_0$ emission bands (which closely corresponds to the respective absorption bands due to the small Stoke's shift usually observed in rare-earth ions). All the possible Stark components of the $^5D_0 \rightarrow {}^7F_1$ (three) are measurable. However, the five Stark components of the $^5D_0 \rightarrow {}^7F_2$ transition are only clearly observable for the lead metaphosphate glass. This behavior would indicate that the widths of the individual Stark components are broader for the barium and zinc metaphosphate glasses. The $^5D_0 \rightarrow {}^7F_{3,4}$ emissions for all of the samples are not completely resolved and also show no excitation-dependent spectral changes hence are not useful in the subsequent discussion.

The energies of the Stark components of the $^7F_1$ and $^7F_2$ multiplets with respect to $^5D_0$ at each excitation are plotted in Figures 6, 7, and 8 as a function of the wavelength ($^5D_0$ excitation energy) for the zinc, barium, and lead metaphosphate glasses, respectively.

IV. DISCUSSION

The emission bands of the spectra obtained for the metaphosphate glasses (Figs. 3, 4, and 5) are characteristic of those produced by other glasses and can be interpreted using crystal-field theory. The crystal-field Hamil-

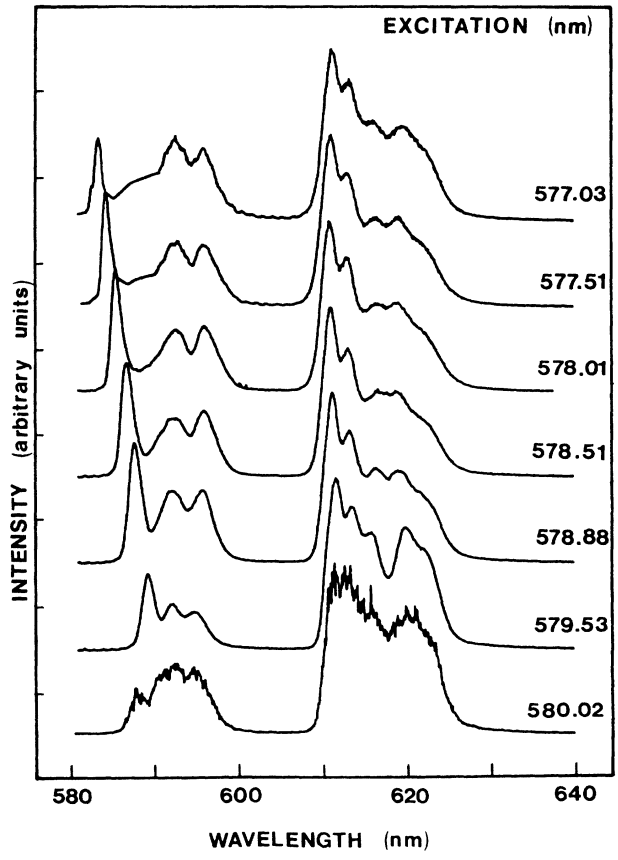

FIG. 5. Emission spectra of Eu^{3+} in $Pb(PO_3)_2$ glass at 77 K using different excitation wavelengths.

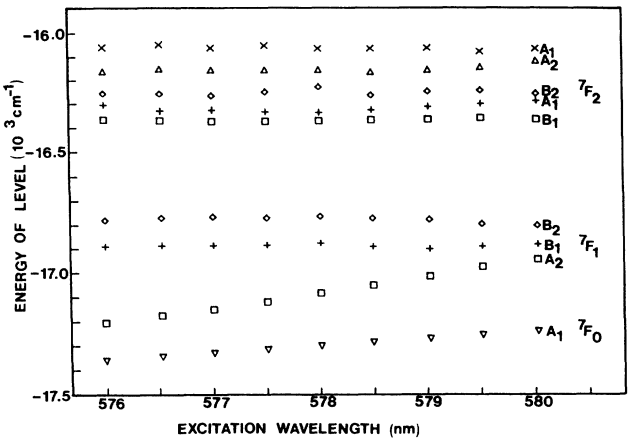

FIG. 6. Energy of the Stark components of the $^7F_0$, $^7F_1$, and $^7F_2$ emissions of Eu^{3+} in $Ba(PO_3)_2$ glass relative to the $^5D_0$ emitting level at each excitation as a function of excitation wavelength.

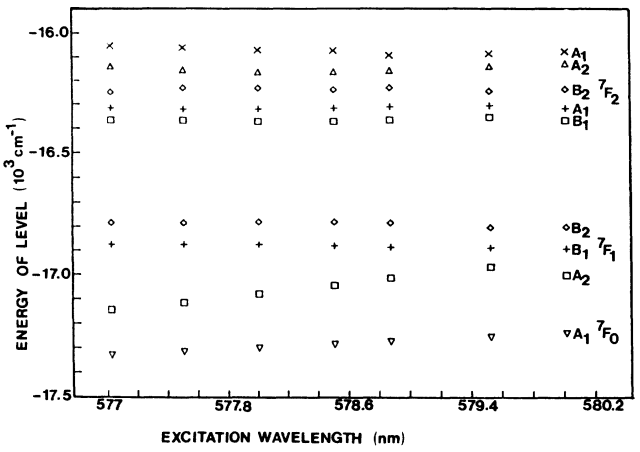

FIG. 8. Energy of the Stark components of the $^7F_0$, $^7F_1$, and $^7F_2$ emissions of Eu^{3+} in $Pb(PO_3)_2$ glass relative to the $^5D_0$ emitting level at each excitation as a function of excitation wavelength.

tonian ($\mathcal{H}_c$) is most conveniently written in its operator equivalent form [16]

$$\mathcal{H}_c + \sum_n \sum_m \theta_j^n \left[B_{nm}^c O_{nm}^c + B_{nm}^s O_{nm}^s \right] , \tag{3}$$

where

$$B_{nm}^{c,s} \langle r \rangle = A_{nm}^{c,s} \langle r \rangle = -|e| K_n \langle r^n \rangle \gamma_{nm}^{c,s}$$

are the crystal-field parameters; $O_{nm}^{c,s}$ are the operator equivalent expressions, θ_n^n is the operator equivalent factor α_j, β_j or γ_j; K_n is the normalizing factor and $\gamma_{nm}^{c,s}$ are lattice sums. The various entries in the secular determinant are

$$< JM|\mathcal{H}_c|JM' > = \mathcal{H}_{MM'} \tag{4}$$

and are easily evaluated from published tables.[16] As has been done for oxide and fluoride glasses,[1-3,21] the crystal field calculations are based on the assumption that the symmetry around the Eu^{3+} ions is C_{2v}. This is the highest symmetry for which full splitting of the $^7F_1$ and $^7F_2$ levels of Eu^{3+} is allowed and the lowest for which symmetry distinction of most of the components is maintained. Using the equations of Lempicki *et al.*,[16] a set of crystal-field parameters, B_{nm}, giving the best fit to all eight components were derived for each spectrum for the three glasses studied. The symmetry assignments of Brecher and Riseberg[3] simulate the experimental energy scheme in a satisfactory way with very good root-mean-square (rms) deviations between the fitted and observed peak positions. The pertinent crystal-field parameters as a function of excitation wavelength are shown in Figs. 9, 10, and 11.

To understand the structural implications of these re-

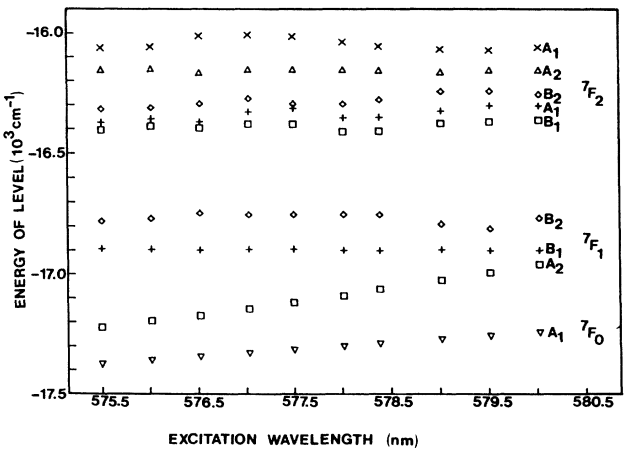

FIG. 7. Energy of the Stark components of the $^7F_0$, $^7F_1$, and $^7F_2$ emissions of Eu^{3+} in $Zn(PO_3)_2$ glass relative to the $^5D_0$ emitting level at each excitation as a function of excitation wavelength.

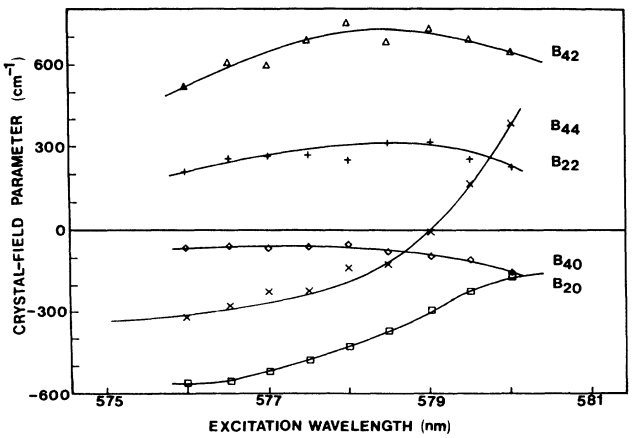

FIG. 9. Observed crystal-field parameters ($B_{20}=\square$, $B_{22}=+$, $B_{40}=\Diamond$, $B_{42}=\triangle$, $B_{44}=\times$) for Eu^{3+} doped $Ba(PO_3)_2$ glass.

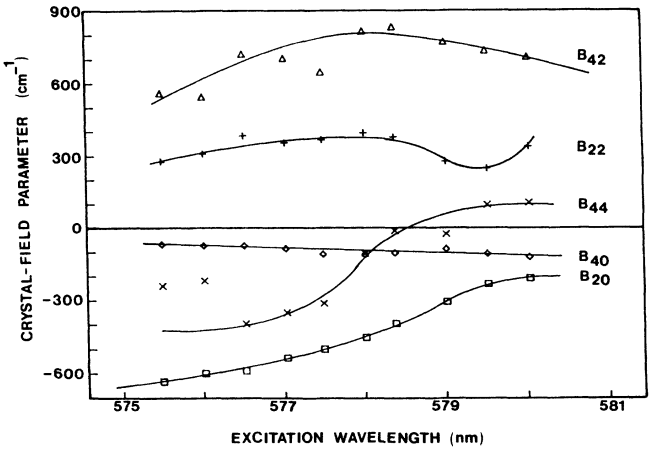

FIG. 10. Observed crystal-field parameters ($B_{20}=\square$, $B_{22}=+, B_{40}=\Diamond$, $B_{42}=\triangle$, $B_{44}=\times$) for Eu^{3+} doped $Zn(PO_3)_2$ glass.

sults a model for the arrangement of ligands surrounding the emitting ion is required. A suitable structural model for the coordination in oxide glasses has been developed by Brecher and Riseberg.[3] We shall examine this model for its applicability to the metaphosphate glass system. This model limits its consideration to the immediate environment of the Eu^{3+} ion, and it involves eight equidistant coordinating oxygens arranged in a distorted antiprism with C_{2v} symmetry into which a ninth coordinator (oxygen) intrudes along the C_2 axis. The assumption that the europium is eightfold or ninefold coordinated is not unreasonable if we consider the ubiquitousness of such coordination in crystalline rare-earth compounds and the absence of chemical or structural constraints that that might prevent the rare earth from achieving its maximum coordination.[19]

We found that Brecher and Riseberg's model[3] gave reasonable agreement to the observed changes both in magnitude and sign: B_{20} increases by a factor of 2, 3.1, and 3.4 for the lead, zinc, and barium metaphosphate glasses, respectively. B_{40} changes relatively little, and B_{44} shows a sharp increase accompanied by a change of sign. While the signs for B_{20}, B_{40}, and B_{44} are uniquely determined by the spectral assignments and must be satisfied, those for B_{22} and B_{42} are essentially arbitrary.

Pure orientational information about the coordination can be extracted by considering the ratios of the crystal-field parameters $-B_{22}/B_{20}$ and B_{44}/B_{40}. The theoretical ratios of Brecher and Riseberg[3] and those determined for the metaphosphate glasses are plotted in Fig. 12. The points determined in this study follow the theoretical ones quite well (shape of the curve) indicating the presence of sites covering the full range of eight to nine coordination. However, we observe that the experimental points do not fall on the line predicted by the model but are displaced downward.

Seeking a suitable explanation for the fact that the experimental points are displaced downward from the theoretical points, we considered the structural modifications possible within the context of changing the network modifying ion, and on the local fields at the Eu^{3+} sites. In metaphosphate glasses each phosphorus-oxygen tetrahedron is linked to two other tetrahedra and one oxygen per tetrahedron with a metal ion. This structure leads to the existence of long chains of tetrahedra,

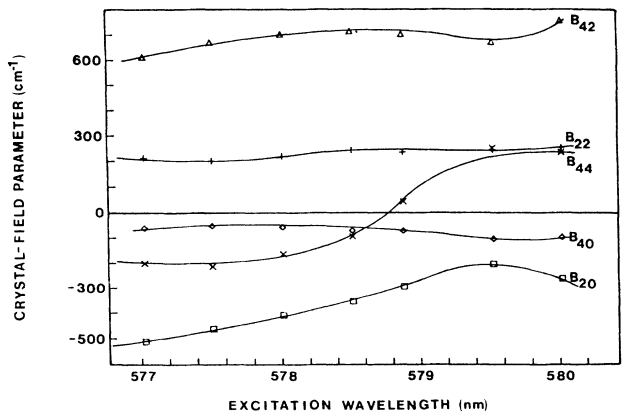

FIG. 11. Observed crystal-field parameters ($B_{20}=\square$, $B_{22}=+, B_{40}=\Diamond$, $B_{42}=\triangle$, $B_{44}=\times$) for Eu^{3+} doped $Pb(PO_3)_2$ glass.

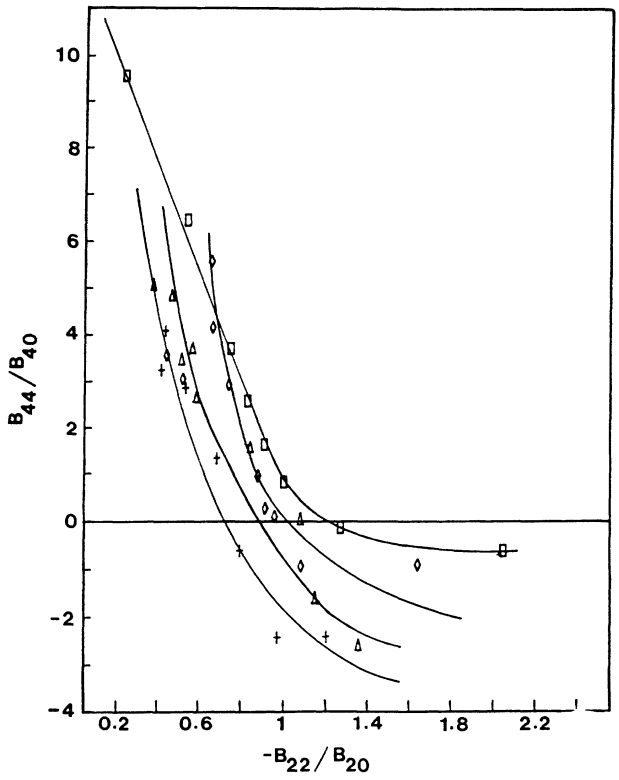

FIG. 12. Behavior of major crystal-field ratios $-B_{22}/B_{20}$ and B_{44}/B_{40}. The line and $\square$ symbols represent values calculated from the geometric model [Brecher and Riseberg (Ref. 3)]. The symbols $\triangle$, $\Diamond$, $+$ indicate the experimental values for $Ba(PO_3)_2$, $Zn(PO_3)_2$, and $Pb(PO_3)_2$, respectively.

TABLE IV. Measured intensity ratios, $I(^5D_0 \rightarrow {}^7F_2)/I(^5D_0 \rightarrow {}^7F_1)$, peak fluorescence wavelengths, λ_p, and crystal-field strengths (S) for Eu^{3+} in $Zn(PO_3)_2$, $Pb(PO_3)_2$, and $Ba(PO_3)_2$ glasses.

	$I(^5D_0 \rightarrow {}^7F_2)/I(^5D_0 \rightarrow {}^7F_1)$	λ_p (nm)	Average crystal-field strength (S) (cm^{-1})
$Zn(PO_3)_2$	3.88	578.37	389
$Ba(PO_3)_2$	3.16	578.59	356
$Pb(PO_3)_2$	2.08	578.88	351

where the long chain phosphate molecules are entwined, and the introduction of the Eu^{3+} ions causes cross linking of the phosphate structure.[20] If we consider the network modifiers (Ba, Zn, and Pb) to be incorporated between the long chain phosphate molecules in the vicinity of the Eu^{3+} ion, then the symmetry and/or covalency of the glass at the Eu^{3+} should be different for the different modifiers. The differences in Eu^{3+} emission spectra as a function of glass composition can be properly described by the intensity ratios[7]

$$I(^5D_0 \rightarrow {}^7F_2)/I(^5D_0 \rightarrow {}^7F_1)$$

and

$$I(^5D_0 \rightarrow {}^7F_4)/I(^5D_0 \rightarrow {}^7F_1) ,$$

which are related to the Judd-Ofelt parameters Ω_2 and Ω_4. The Judd-Ofelt parameter Ω_2 is related to the covalency and/or structural changes in the vicinity of the Eu^{3+} ion (short-range effect) and Ω_4 is related to the long-range effects. We observe for the Eu^{3+} doped phosphate glasses, that the ratios (Table IV),

$$I(^5D_0 \rightarrow {}^7F_2)/I(^5D_0 \rightarrow {}^7F_1)$$

for the barium and zinc metaphosphate glasses are 3.16 and 3.88, respectively. The larger modifier ion (Ba^{2+}, ionic radii, 1.56 Å) gives rise to a larger average distance between the phosphate chains which results in the average Eu-O distance to increase, therefore producing a weaker field around the Eu^{3+} ion. This manifests itself as a decrease in the value of

$$I(^5D_0 \rightarrow {}^7F_2)/I(^5D_0 \rightarrow {}^7F_1) .$$

In the case of the lead metaphosphate glass, the decrease in

$$I(^5D_0 \rightarrow {}^7F_2/(I^5D_0 \rightarrow {}^7F_1)$$

cannot be accounted for in terms of the ionic radii ($Ba^{2+}=1.56$ Å, $Pb^{2+}=1.43$ Å) but rather that the Pb^{2+} ion is more strongly bonded to the oxygen which reduces the covalency of the Eu—O bond.[22]

Further support for the arguments presented above is derived from the fact that the energy of the transition $^5D_0 \rightarrow {}^7F_0$ (λ_p peak emission) is lower for the lead metaphosphate glass (Table IV). Weber *et al.*[23] have suggested that a reduced nephelauxetic effect shifts the center of gravity of the J states to higher energies which appears as a small lowering of λ_p. One can also consider the crystal-field strength parameter for the three metaphosphate glasses studied. The crystal-field strength parameter (S) was calculated using the relationship[24]

$$S=\left[\tfrac{1}{3}\sum_k \frac{1}{2k+1}\left[B_{ko}^2+2\sum_{m>0}(RB_{km}^2+IB_{km}^2)\right]\right] . \quad (5)$$

The resulting values, (average) obtained are given in Table IV. The crystal-field strength parameter decreases in the order $S_{Pb} < S_{Ba} < S_{Zn}$ giving further support to the role that the modifier ion plays in changing the local field at the Eu^{3+} sites.

The crystal-field parameter B_{20} is particularly sensitive to the magnitude of the electrostatic interactions. The lattice dependent portion of B_{20} (in Cartesian coordinates) is given by

$$B_{20} \propto \frac{(3z^2-r^2)}{r^3} . \quad (6)$$

Roughly speaking then, larger (in magnitude) values of B_{20} imply that the coordinating ligands are closer to the Eu^{3+}. For the Pb metaphosphate glass the values of B_{20} are in fact smaller than those found for barium and zinc metaphosphate. This is consistent with the interpretation that we have presented.

The influence of the network modifier ions on the major crystal-field parameter ratio plot (Fig. 12) can now be considered. The differences in the plot (downward shift) can be attributed to (i) the differences in the ionic radii of Ba^{2+} and Zn^{2+} and (ii) the strength of the Pb—O bond. Both factors affect the Eu—O bond, therefore the degree of the downward shift can be related to the effective crystal field at the Eu^{3+} ion. In the case of Ba^{2+} and Zn^{2+}, the Eu^{3+} ion in the barium metaphosphate glass will feel a weaker field since the phosphate chains are further apart and consequently the Eu—O bond is longer. As we mentioned previously, in the lead metaphosphate glass the predominant factor that affects the field at the Eu^{3+} ion is the reduced covalency of the Eu—O bond. Thus, the model as in the case of oxide glasses[1,2] is chemically consistent and gives reasonable agreement to the spectroscopically derived parameter.

V. CONCLUSIONS

The present work has yielded a reasonably complete picture of the spectroscopic behavior of Eu^{3+} in metaphosphate glasses. The structural model of Brecher and Riseberg was applied and it described the overall properties (structure and bonding) of the metaphosphate glasses in a reasonable fashion. We showed that major crystal-field parameter ratios can be used to obtain information regarding the properties of the chemical bonding.

ACKNOWLEDGMENTS

The authors gratefully acknowledge the Natural Science and Engineering Research Council of Canada and the Faculty of Arts and Science of Concordia University for financial support. We also acknowledge the financial support of the Italian Ministry of Education.

[1]J. A. Capobianco, T. F. Belliveau, G. Lord, D. J. Simkin, J. Tait, and P. J. Hayward, Phys. Rev. B **34**, 4204 (1986).
[2]J. A. Capobianco, P. P. Proulx, and N. Raspa, Chem. Phys. Lett. **160**, 591 (1989).
[3]C. Brecher and L. A. Riseberg, Phys. Rev. B **13**, 81 (1976).
[4]C. Brecher, L. A. Riseberg, and M. J. Weber, Phys. Rev. B **18**, 5799 (1978).
[5]J. Hegarty, W. M. Yen, and M. J. Weber, Phys. Rev. B **18**, 5816 (1978).
[6]J. Hegarty, W. M. Yen, M. J. Weber, and D. H. Blackburn, J. Lumin. 18& 19, 657 (1979).
[7]E. W. J. L. Oomen and A. M. A. Van Dongen, J. Non-Cryst. Solids **111**, 205 (1989).
[8]C. K. Jorgensen and B. R. Judd, Mol. Phys. **8**, 291 (1964).
[9]R. D. Peacock, Struct. Bonding (Berlin) **22**, 83 (1975).
[10]R. Reisfeld and N. Lieblich, J. Phys. Chem. Solids **34**, 1467 (1973).
[11]R. Reisfeld, L. Boehn, M. Ish-Shalom, and R. Fisher, Phys. Chem. Glasses **15**, 76 (1974).
[12]R. Reisfeld and C. K. Jorgensen, in *Handbook on the Physics and Chemistry of Rare Earth,* edited by K. A. Gschneidner and L. Eyring (North-Holland, Amsterdam, 1987), Chap. 58.
[13]M. J. Weber (unpublished).
[14]T. F. Belliveau, Ph.D. thesis, McGill University, 1988.
[15]D. W. Marquardt, J. Soc. Ind. Appl. Math. **11**, 43 (1963).
[16]A. Lempicki, H. Samelson, and C. Brecher, J. Mol. Spectrosc. **27**, 375 (1968).
[17]B. R. Judd, Phys. Rev. **127**, 750 (1962).
[18]G. S. Ofelt, J. Chem. Phys. **37**, 511 (1962).
[19]M. J. Weber, in *Optical Properties of Ions in Crystal,* edited by H. M. Crosswhite and H. W. Moos (Interscience, New York, 1967), p. 467.
[20]W. T. Carnall, P. R. Fields, and K. Rajnak, J. Chem. Phys. **49**, 4450 (1968).
[21]C. Brecher and L. A. Riseberg, Phys. Rev. B **21**, 2607 (1980).
[22]M. J. Weber, L. A. Boatlier, and B. C. Sales, J. Non-Cryst. Solids **74**, 167 (1985).
[23]M. J. Weber, R. A. Saroyan, and R. C. Ropp, J. Non-Cryst. Solids **44**, 137 (1981).
[24]N. C. Chang, J. B. Gruber, R. P. Leavitt, and C. A. Morrison, J. Chem. Phys. **78**, 3877 (1982).